

Design procedure for photonic crystal fibers with ultra-flattened chromatic dispersion

Huizhen Xu (徐惠真)^{1,2*}, Jian Wu (伍 剑)¹, Yitang Dai (戴一堂)¹,
Cong Xu (徐 聪)¹, and Jintong Lin (林金桐)¹

¹Key Laboratory of Information Photonics and Optical Communications (Beijing University of Posts and Telecommunications), Ministry of Education, Beijing 100876, China

²College of Science, Jimei University, Xiamen 361021, China

*Corresponding author: elimshee@gmail.com

Received November 1, 2010; accepted December 14, 2010; posted online April 18, 2011

A simple design procedure is used to generate photonic crystal fibers (PCFs) with ultra-flattened chromatic dispersion. Only four parameters are required, which not only considerably saves the computing time, but also distinctly reduces the air-hole quantity. The influence of the air-hole diameters of each ring of hexagonal PCFs (H-PCF, including 1-hole-missing and 7-hole-missing H-PCFs), circular PCFs (C-PCF), square PCFs (S-PCF), and octagonal PCFs (O-PCF) is investigated through simulations. Results show that regardless of the cross section structures of the PCFs, the 1st ring air-hole diameter has the greatest influence on the dispersion curve followed by that of the 2nd ring. The 3rd ring diameter only affects the dispersion curve within longer wavelengths, whereas the 4th and 5th rings have almost no influence on the dispersion curve. The hole-to-hole pitch between rings changes the dispersion curve as a whole. Based on the simulation results, a procedure is proposed to design PCFs with ultra-flattened dispersion. Through the adjustment of air-hole diameters of the inner three rings and hole-to-hole pitch, a flattened dispersion of 0 ± 0.5 ps/(nm·km) within a wavelength range of 1.239–2.083 μm for 5-ring 1-hole-missing H-PCF, 1.248–1.992 μm for 5-ring C-PCF, 1.237–2.21 μm for 5-ring S-PCF, 1.149–1.926 μm for 5-ring O-PCF, and 1.294–1.663 μm for 7-hole-missing H-PCF is achieved.

OCIS codes: 060.2280, 220.4000, 060.4005.

doi: 10.3788/COL201109.050603.

Since photonic crystal fibers (PCFs) were first reported in 1996^[1], different kinds of PCF cross section structures, such as hexagonal PCF (H-PCF)^[2], octagonal PCF (O-PCF)^[3], square PCF (S-PCF)^[4], and so on, have been developed. The dispersion properties of PCFs are significantly different from those of conventional fibers because the cross section structures consisting of an array of air holes allow for flexible tailoring of the dispersion curves, which cannot be realized in conventional optical fibers. Control of the chromatic dispersion in PCFs is of huge importance for applications in optical fiber communications^[5], dispersion compensation, supercontinuum generation^[6,7], and so on.

Many PCF designs have been proposed to achieve ultra-flattened chromatic dispersion. In Ref. [8], the chromatic dispersion in conventional PCFs was controlled by changing the air holes, which are arrayed in a regular hexagonal structure with the same diameters in the cladding region. A PCF with a dispersion of 0 ± 0.6 ps/(nm·km) from 1.24 to 1.44 μm was realized. Because the air-filling fraction is too small to realize ultra-flattened dispersion, more than 20 rings of air holes (up to 455 holes) are required to significantly reduce the confinement loss, thereby causing extreme complexity in the manufacturing process. Moreover, the achievement of this kind (same air-hole size) of ultra-flattened dispersion over such a large wavelength range involves highly accurate control of air-hole diameter and pitch^[9]. To reduce the quantity of air holes and realize ultra-flattened dispersion, many designs discussed in literature have the following characteristics: differently spaced rings of holes^[3] and different sizes of holes^[10]. In Ref. [3], the authors

presented an 8-ring O-PCF. After optimization of the diameters of the 1st ring, the outer seven rings, and the air-hole pitch, PCFs with a dispersion of 0 ± 0.5 ps/(nm·km) in a wavelength range of 1.46–1.66 μm were obtained. In Ref. [10], a new design with four or five rings of gradually increasing air-hole diameters for each ring was proposed for achieving ultra-flattened dispersion. Through optimization, a four-ring PCF with a flattened dispersion of 0 ± 0.5 ps/(nm·km) for a wavelength of 1.19–1.69 μm , and a five-ring PCF with a flattened dispersion of 0 ± 0.4 ps/(nm·km) for a wavelength 1.23–1.72 μm were proposed. This design considerably reduces the ring number of air holes, but the design procedure becomes complicated because several geometrical parameters, five (four air-hole diameters and one pitch) for the four-ring PCF and six (five air-hole diameters and one pitch) for the five-ring type, are needed to simultaneously optimize dispersion properties. Several studies have already used the genetic algorithm to determine global minima for ultra-flattened design^[11,12]. However, the genetic algorithm entails considerable computing time because it requires numerous iterations. In Ref. [12], for example, the algorithm required 40 individuals and 13 generations.

In this letter, a simple procedure for different kinds of PCFs is presented to obtain ultra-flattened dispersion. This design procedure requires only four parameters (three air-hole diameters and one hole-to-hole pitch), considerably saving the computing time. In addition, it requires only one array layout cross section structure and four or five rings of air holes, tremendously reducing the complexity in manufacturing process. This design procedure is suitable not only for 1-hole-missing PCFs

(including conventional H-PCFs, C-PCFs, S-PCFs, and O-PCFs), but also for 7-hole-missing PCFs, which are large-mode-area fibers.

To improve dispersion properties and reduce operational complexity, a simple design procedure was used for dispersion control. Figure 1 shows the cross sections of H-PCF, C-PCF, S-PCF, O-PCF, and 7-hole-missing H-PCF with uniform air holes that are taken into consideration. These four kinds of PCFs have a two-dimensional (2D) silica core and five air-silica cladding rings. In the figure, d_n ($n=1-5$) is the air-hole diameter of the N th air-hole ring; Λ is the hole-to-hole pitch for H-PCF, S-PCF, and the air-hole pitch between rings for C-PCF and O-PCF. During the simulations, the beam propagation method (BPM)^[13] was used to calculate the dispersion curves of the PCFs. The BeamPROP module of the commercial software package RSoft (RSoft Design Group, New York) was used for the simulations. The iterative function method^[14] was used to obtain modal characteristics. During the simulations, the transparent boundary condition^[15] was adopted. The simulations were performed in a window of $12 \times 12 \mu\text{m}$ within the transverse x - y plane of the PCF, in steps of $\Delta z = 0.1 \mu\text{m}$ and $\Delta x = \Delta y = 0.05 \mu\text{m}$. The tolerance for n_{eff} convergence was as low as 1×10^{-7} to guarantee numerical precision. The refractive index of silica is given by the Sellmeier dispersion equation^[16]:

$$n_m^2(\lambda) = 1 + \sum_{i=1}^l \frac{A_i \lambda^2}{\lambda^2 - \lambda_i^2}. \quad (1)$$

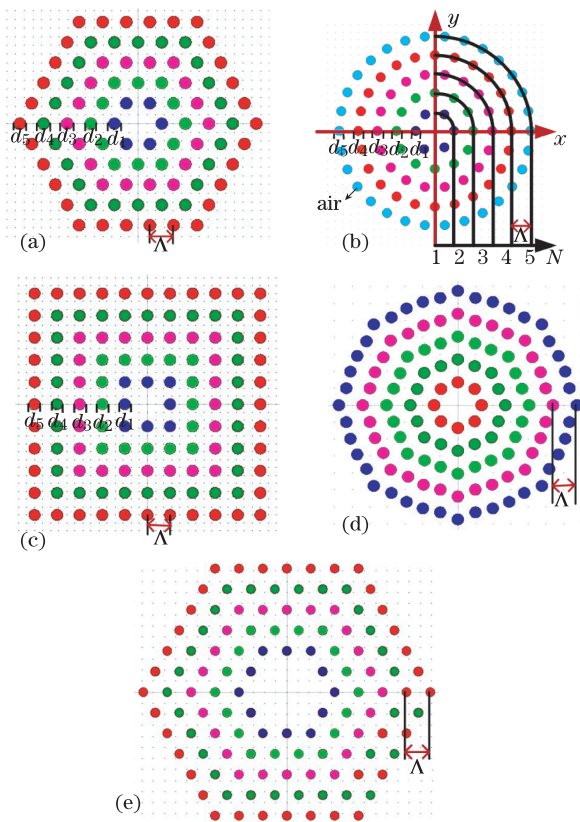


Fig. 1. Cross sections of 5-ring (a) H-PCF, (b) C-PCF, (c) S-PCF, (d) O-PCF with uniform air holes, and (e) 7-hole-missing H-PCF.

Defining n_{eff} as the effective index of fundamental mode, which takes material dispersion and waveguide dispersion into account, chromatic dispersion D ^[17] can be obtained as

$$D = -\frac{\lambda}{c} \frac{d^2 \text{Re}(n_{\text{eff}})}{d\lambda^2}, \quad (2)$$

where c is the velocity of light in vacuum, and Re stands for the real part. Confinement loss L_c can be calculated from the imaginary component of the fundamental mode index by^[12]:

$$L_c(\text{dB/km}) = 8.686 k_0 \text{Im}[n_{\text{eff}}] \times 1,000, \quad (3)$$

where k_0 is the free space wave number and equals $2\pi/\lambda$. Local air filling fraction f_n is defined as d_n/Λ . In the subsequent simulations, the dispersion curves are not shown in the figures when the fundamental mode is no longer the guide mode in the PCFs.

H-PCFs are the most conventional type of PCF structures and are the most widely used. We first took this fact into consideration. The influence of the air-hole diameters of each ring on the dispersion profile was investigated. The local air-filling fractions $f_1 - f_5$ were varied from 0.2 to 0.8 with an increment of 0.2, and Λ was set to $2 \mu\text{m}$. Figure 2 shows the influence of the 1st–4th rings on the dispersion curves. The influence of f_5 is not shown because its simulation results are nearly the same as those of f_4 .

Figure 2 clearly shows that the 1st ring air holes have the greatest influence on chromatic dispersion. These affect the dispersion curve within the entire wavelength range that is taken into consideration. In Fig. 2(a), within the shorter wavelength range, dispersion value increases when f_1 increases, whereas the curve shape changes minimally. Within the longer wavelength range, the dispersion curve shape markedly changes with the variation of f_1 . For the curves of $f_1 = 0.2$ and 0.4 , the dispersion slopes are positive within the entire wavelength range; whereas for the curves of $f_1 = 0.6$ and 0.8 , the slopes change from positive to negative. As shown in Fig. 2(b), the variation of f_2 has less influence on dispersion values than that in f_1 . Moreover, f_2 has a much greater influence on the dispersion curve within the longer wavelength range than within the shorter wavelength range. The dispersion value decreases with decreasing f_2 . Figure 2(c) shows that f_3 has little effect on the dispersion curve. The curves almost overlap

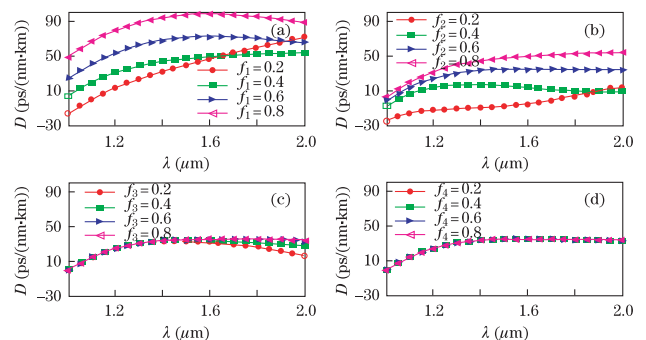


Fig. 2. Influence of $f_1 - f_4$ on chromatic dispersion D of H-PCF. (a) $\Lambda = 2 \mu\text{m}$, $f_2 = f_3 = f_4 = f_5 = 0.8$; (b) $\Lambda = 2 \mu\text{m}$, $f_1 = 0.4$, $f_3 = f_4 = f_5 = 0.8$; (c) $\Lambda = 2 \mu\text{m}$, $f_1 = 0.4$, $f_2 = 0.6$, $f_4 = f_5 = 0.8$; (d) $\Lambda = 2 \mu\text{m}$, $f_1 = 0.4$, $f_2 = 0.6$, $f_3 = f_5 = 0.8$.

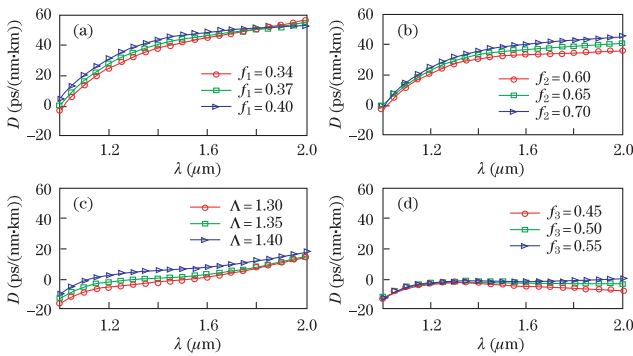


Fig. 3. Design procedure for H-PCF with ultra-flattened dispersion. (a) $\Lambda = 2 \mu\text{m}$, $f_2 = f_3 = 0.8$, $f_4 = f_5 = 0.95$; (b) $\Lambda = 2 \mu\text{m}$, $f_1 = 0.37$, $f_3 = 0.8$, $f_4 = f_5 = 0.95$; (c) $f_1 = 0.37$, $f_2 = 0.65$, $f_3 = 0.8$, $f_4 = f_5 = 0.95$; (d) $\Lambda = 1.35 \mu\text{m}$, $f_1 = 0.37$, $f_2 = 0.65$, $f_4 = f_5 = 0.95$.

with each other within the shorter wavelength range when f_3 varies. f_3 only slightly affects the dispersion curves within the longer wavelength range. As shown in Fig. 2(d), f_4 and f_5 have no influence on the dispersion profile.

In accordance with the simulation results above, a simple design procedure was used to control dispersion properties. Because only the air-hole diameters of the inner three rings influence the dispersion curves, only the three parameters need to be changed without regard for the 4th and 5th rings' air-hole diameters. The large values of f_4 and f_5 are beneficial to better confinement of PCFs^[10,18], although they have no influence on the dispersion profile. Therefore, f_4 and f_5 were set to 0.95 and remained unchanged during the subsequent simulations. Figure 3 shows the design procedure. Figure 2(a) shows that when $f_1 = 0.4$, the dispersion curve flattens within the longer wavelength range. Therefore, f_1 was varied from 0.34 to 0.4 to determine a more suitable value. Figure 3(a) shows that although the dispersion value of curve $f_1 = 0.37$ is nearly the same as that of curve $f_1 = 0.4$ within the longer wavelength range, the former is smaller within the shorter wavelength range. The curve slope of $f_1 = 0.34$ is more steep than those of the other two. Therefore, $f_1 = 0.37$ was chosen for the next optimization. Next, f_2 was varied to optimize the dispersion profile within medium and longer wavelength ranges. Figure 3(b) illustrates that

the decrease in f_2 reduces the dispersion value and flattens the curves more than that in Fig. 3(a) within about 1.4–2.0 μm wavelengths. However, the flattened dispersion values are much higher than zero. To generate a dispersion value near zero, the pitch Λ is modified. Figure 3(c) clearly shows that changing Λ while keeping all other parameters constant changes the curve as a whole. In addition, the dispersion value of the entire curve decreases as Λ decreases. For $\Lambda = 1.35 \mu\text{m}$, the dispersion value is near zero between about 1.2 and 1.8 μm wavelengths. However, the curve is still a little steep within longer wavelengths. In the last section, f_3 only slightly affects the dispersion curve within the longer wavelength range. Therefore, f_3 was varied to flatten the longer wavelength range. Figure 3(d) shows that the dispersion value decreases with decreasing f_3 . The curve of $f_3 = 0.5$ is much flatter within the longer wavelength range than the other two curves. Finally, through fine adjustments in the four parameters (inner three rings' air-hole diameters and pitch), an ultra-flattened dispersion wavelength within broader wavelengths is obtained.

C-PCFs have been discussed in our previous work^[19], in which we concluded that the influence of air-hole diameter on the dispersion curve gradually weakened from the inside ring to the outside. Through the same procedure as H-PCF, 4-ring and 5-ring C-PCFs with ultra-flattened dispersion are obtained.

The cross section of S-PCF with uniform air holes is shown in Fig. 1(c). After the investigation on the variation in each ring air-hole diameter, we found that they had the same influence on the dispersion curve as H-PCF and C-PCF did. Therefore, S-PCF with ultra-flattened dispersion can be obtained using the same procedure.

Razzak *et al.* proposed an O-PCF for ultra-flattened dispersion and obtained a dispersion of $0 \pm 0.5 \text{ ps}/(\text{nm}\cdot\text{km})$ in a wavelength range^[3] of 1.46–1.66 μm . The same procedure was applied to O-PCF in the simulations, and ultra-flattened dispersion was finally obtained.

The design and discussion above are limited to 1-hole-missing PCFs. Now we extend our conclusion to 7-hole-missing H-PCFs, which are large mode area fibers. After using the same design procedure, ultra-flattened dispersion can be achieved. However, the wavelength range with flattened dispersion is narrower than that in 1-hole-missing PCF due to its large high-index core.

Table 1. PCFs with Ultra-Flattened Dispersion

	Geometrical Parameters	Flattened Dispersion Wavelength Range (μm)		
		$0 \pm 0.25 \text{ ps}/(\text{nm}\cdot\text{km})$	$0 \pm 0.4 \text{ ps}/(\text{nm}\cdot\text{km})$	$0 \pm 0.5 \text{ ps}/(\text{nm}\cdot\text{km})$
5-Ring H-PCF	$\Lambda = 1.34 \mu\text{m}$, $f_1 = 0.37$, $f_2 = 0.66$, $f_3 = 0.51$, $f_4 = f_5 = 0.95$	1.265–1.985	1.248–2.048	1.239–2.083
4-Ring C-PCF	$\Lambda = 1.58 \mu\text{m}$, $f_1 = 0.39$, $f_2 = 0.68$, $f_3 = 0.42$, $f_4 = 0.98$	1.230–1.789	1.219–1.816	1.212–1.830
5-Ring C-PCF	$\Lambda = 1.5 \mu\text{m}$, $f_1 = 0.39$, $f_2 = 0.74$, $f_3 = 0.3$, $f_4 = f_5 = 0.96$	1.249–1.990	1.248–1.991	1.248–1.992
5-Ring S-PCF	$\Lambda = 1.4 \mu\text{m}$, $f_1 = 0.4$, $f_2 = 0.7$, $f_3 = 0.3$, $f_4 = f_5 = 0.95$	–	1.244–2.195	1.237–2.21
5-Ring O-PCF	$\Lambda = 1.42 \mu\text{m}$, $f_1 = 0.35$, $f_2 = 0.67$, $f_3 = 0.29$, $f_4 = f_5 = 0.7$	–	1.149–1.926	1.149–1.926
7-Hole-Missing H-PCF	$\Lambda = 0.81 \mu\text{m}$, $f_1 = 0.4$, $f_2 = 0.5$, $f_3 = 0.39$, $f_4 = f_5 = 0.95$	–	1.307–1.654	1.294–1.663

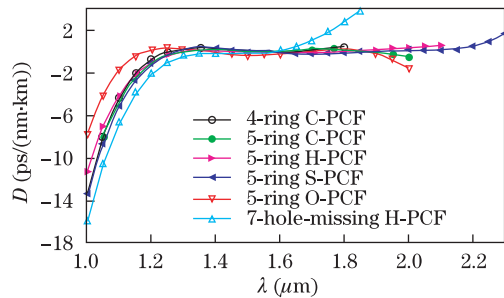


Fig. 4. Dispersion of 4-ring C-PCF, 5-ring C-PCF, 5-ring H-PCF, 5-ring S-PCF, 5-ring O-PCF, and 7-hole-missing H-PCF.

Through the optimization procedure above, PCFs with ultra-flattened dispersion are obtained. Table 1 lists the geometrical parameters. In the flattened dispersion wavelength range of the 1-hole-missing H-PCF, C-PCF, S-PCF, O-PCF, and 7-hole-missing H-PCF, we used the proposed design procedure. Figure 4 shows the chromatic dispersion of these six PCFs. Compared with the abovementioned references, the flattened dispersion wavelength ranges of these PCFs are precisely broadened through the design procedure.

The optimization process for PCFs with ultra-flattened dispersion can be summarized as follows.

Step 1. The air-hole diameter values of the outer rings (except the inner three rings) are set to a larger value for better confinement. Then, the air filling fraction of the 1st ring is scanned to determine a relatively flat dispersion curve.

Step 2. The air filling fraction of the 2nd ring is scanned, and the variation in f_2 flattens the dispersion curve to a greater extent within the longer wavelength range.

Step 3. The adjustment of the hole-to-hole pitch causes the dispersion curve to move as a whole. The curve near zero is then moved through the change of Λ .

Step 4. Finally, the dispersion value within the longer wavelength range can be improved through adjustment in the air filling fraction of the 3rd ring.

In conclusion, the influence of air-hole diameters on the dispersion curve is investigated for conventional H-PCFs (including 1-hole-missing and 7-hole-missing), C-PCFs, S-PCFs, and O-PCFs. Regardless of the kind of PCF cross section structure, the influence of air-hole diameters on dispersion curves is similar. The 1st ring air-hole diameter has the greatest influence on the dispersion curve, affecting the dispersion curve within the entire wavelength range considered. Within the shorter wavelength range, the dispersion value decreases as f_1 decreases, whereas the curve shape changes minimally. However, within the longer wavelength range, the variation in f_1 affects not only the dispersion value but also the curve shape. The 2nd ring air-hole diameter more considerably affects the dispersion curve within the longer wavelength range than within the shorter wavelength range, whereas the 3rd ring has only minimal influence on the dispersion curve within the longer wavelength range. The 4th and 5th rings' air-hole diameters have almost no influence on the dispersion curve but play an important role in confinement loss. According to the diverse effects of different ring air-hole diameters on the dispersion curve, a design procedure is used to achieve ultra-flattened dispersion. The air-hole diameters of the inner three rings

and the pitch are scanned to search for minima in each step. Through the proposed procedure, a flattened dispersion of 0 ± 0.5 ps/(nm-km) within a wavelength range of $1.239 - 2.083$ μm for 5-ring 1-hole-missing H-PCF, $1.212 - 1.830$ μm for 4-ring C-PCF, $1.248 - 1.992$ μm for 5-ring C-PCF, $1.237 - 2.21$ μm for 5-ring S-PCF, $1.149 - 1.926$ μm for 5-ring O-PCF, and $1.294 - 1.663$ μm for 7-hole-missing H-PCF is achieved. This design procedure is simple and tremendously saves the computing time. In addition, it requires only four parameters (the air-hole diameters of the inner three rings and the pitch) and considerably reduces the quantity of air-hole rings. The proposed procedure should be useful for PCF design with ultra-flattened dispersion.

This work was supported by the National "863" Program of China (Nos. 2009AA01Z256, 2009AA01Z253, and 2008AA01A331) and the National Natural Science Foundation of China (Nos. 61001121, 60736036, and 61006041).

References

1. J. C. Knight, T. A. Birks, P. St. J. Russell, and D. M. Atkin, *Opt. Lett.* **21**, 1547 (1996).
2. T. A. Birks, J. C. Knight, and P. St. J. Russell, *Opt. Lett.* **22**, 961 (1997).
3. S. M. A. Razzak and Y. Namihira, *IEEE Photon. Technol. Lett.* **20**, 249 (2008).
4. F. Couny, P. J. Roberts, T. A. Birks, and F. Benabid, *Opt. Express* **16**, 20626 (2008).
5. M. D. Nielsen, C. Jacobsen, N. A. Mortensen, J. R. Folkenberg, and H. R. Simonsen, *Opt. Express* **12**, 1372 (2004).
6. B. A. Cumberland, J. C. Travers, S. V. Popov, and J. R. Taylor, *Opt. Express* **16**, 5954 (2008).
7. L. Fang, J. Zhao, and X. Gan, *Chin. Opt. Lett.* **8**, 1028 (2010).
8. W. H. Reeves, J. C. Knight, P. St. J. Russell, and P. J. Roberts, *Opt. Express* **10**, 609 (2002).
9. A. Ferrando, E. Silvestre, J. J. Miret, and P. Andres, *Opt. Lett.* **25**, 790 (2000).
10. K. Saitoh, M. Koshiba, T. Hasegawa, and E. Sasaoka, *Opt. Express* **11**, 843 (2003).
11. M. Pourmahyabadi and S. M. Nejad, in *Proceedings of International Conference on Applied Electronics 2009* 211 (2009).
12. E. Kerrinckx, L. Bigot, M. Douay, and Y. Quiquempois, *Opt. Express* **12**, 1990 (2004).
13. D. Yevick and B. Hermansson, *IEEE J. Quantum Electron.* **26**, 109 (1990).
14. D. Yevick and B. Hermansson, *IEEE J. Quantum Electron.* **25**, 221 (1989).
15. G. R. Hadley, *IEEE J. Quantum Electron.* **28**, 363 (1992).
16. I. H. Malitson, *J. Opt. Soc. Am.* **55**, 1205 (1965).
17. C. Chaudhari, T. Suzuki, and Y. Ohishi, in *Proceedings of OFC 2009 OTuC4* (2009).
18. N. H. Hai, Y. Namihira, S. Kajage, F. Begum, T. Kinjo, and S. M. A. Razzak, in *Proceedings of SBMO/IEEE MTT-S International Microwave and Optoelectronics Conference* 46 (2007).
19. H. Xu, J. Wu, K. Xu, Y. Dai, C. Xu, and J. Lin, "Ultra-flattened chromatic dispersion control for circular photonic crystal fibers" submitted to *J. Opt.*